PREDICTION OF ENVIRONMENTAL IMPACT OF HIGH-ENERGY MATERIALS WITH ATOMISTIC COMPUTER SIMULATIONS

Nandhini Sokkalingam*, Jeffrey J. Potoff
Department of Chemical Engineering, Wayne State University, Detroit, MI 48202

Veera M.Boddu, Stephen W.Maloney
Environmental Processes Branch, Construction Engineering Research Laboratory, ERDC, U.S. Army Corp of Engineers
Champaign, IL 61826

ABSTRACT

In this work, force fields are developed for four compounds categorized by the Army as potential insensitive munitions compounds, which includes, 2,4-dinitroanisole (DNAN), N-methyl-p-nitroaniline (MNA), Dinitropyrazole (DNP) and Nitrotriazolone (NTO). These force fields are used to predict pharmacokinetic properties such as octanol-water partition coefficients and Henry's law constants along with other thermophysical properties such as vapor-liquid equilibria, vapor pressure, critical parameters and normal boiling points.

1. INTRODUCTION

Over the past few years, there has been considerable interest in the development of new Insensitive Munitions (IM) that are highly efficient and relatively safe to operate with low chances of an accidental initiation. They possess higher thermal stability and lower shock sensitivity than traditionally used explosive compounds, such as TNT. Although insensitive to shock, impact or thermal effects, they are still known to perform well. Due to increased environmental and safety concerns, it is necessary to determine how these compounds behave in the environment in terms of bioaccumulation potential and aqueous solubility before being extensively employed in explosive formulations.

Gillett has proposed a "pre-biological screen", which correlates the Henry's law constant (log H), octanol-water partition coefficient (log K_{ow}) and the material half-life to predict which materials have the potential to be problematic if released to the environment (Gillett, 1984). A wide variety of experimental techniques (Sangster, 1997) exist to measure the partition coefficients. An alternative strategy is discussed in this work: the application of atomistic computer simulation to the prediction of partition coefficients and phase behavior. Computer simulation has a few benefits over experiments. Given an accurate intermolecular potential function, it is possible to predict the behavior of a material in the environment before it has been synthesized, allowing for a prescreening of potential candidate molecules. Such a prescreening is expected to lead to cost savings by reducing the pool of candidate molecules for synthesis, and potentially leading to reductions in costs due to remediation efforts near load-and-pack facilities.

In this era of supercomputing, complex processes can be simulated in reasonable time scales with high precision and accuracy across a parallel platform of multiple processors with an accurate molecular model or force field and an appropriate simulation methodology.

The structures of the compounds of interest are shown in Fig. 1.

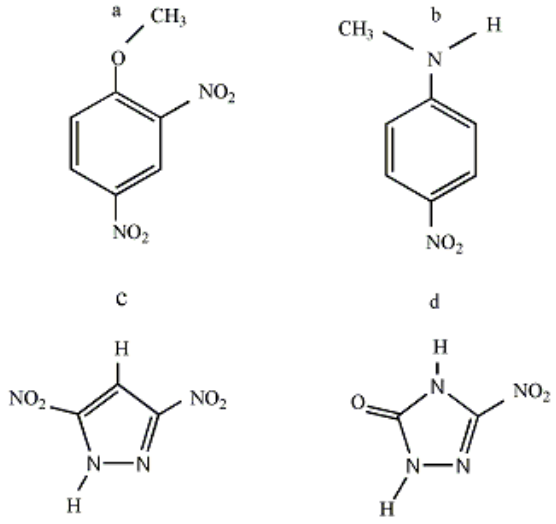

Fig. 1. Structure of the energetic materials. a) DNAN; b) MNA; c) DNP; d) NTO.

2. FORCE FIELD DEVELOPMENT

The accuracy of molecular simulation is dependent entirely on the force fields used to describe the interactions of

Report Documentation Page

Form Approved
OMB No. 0704-0188

1. REPORT DATE	2. REPORT TYPE	3. DATES COVERED
DEC 2008	**N/A**	**-**

4. TITLE AND SUBTITLE	5a. CONTRACT NUMBER
Prediction Of Environmental Impact Of High-Energy Materials With Atomistic Computer Simulations	5b. GRANT NUMBER
	5c. PROGRAM ELEMENT NUMBER
6. AUTHOR(S)	5d. PROJECT NUMBER
	5e. TASK NUMBER
	5f. WORK UNIT NUMBER
7. PERFORMING ORGANIZATION NAME(S) AND ADDRESS(ES) **Department of Chemical Engineering, Wayne State University, Detroit, MI 48202**	8. PERFORMING ORGANIZATION REPORT NUMBER
9. SPONSORING/MONITORING AGENCY NAME(S) AND ADDRESS(ES)	10. SPONSOR/MONITOR'S ACRONYM(S)
	11. SPONSOR/MONITOR'S REPORT NUMBER(S)

12. DISTRIBUTION/AVAILABILITY STATEMENT
Approved for public release, distribution unlimited

13. SUPPLEMENTARY NOTES
See also ADM002187. Proceedings of the Army Science Conference (26th) Held in Orlando, Florida on 1-4 December 2008

14. ABSTRACT

15. SUBJECT TERMS

16. SECURITY CLASSIFICATION OF:			17. LIMITATION OF ABSTRACT	18. NUMBER OF PAGES	19a. NAME OF RESPONSIBLE PERSON
a. REPORT	b. ABSTRACT	c. THIS PAGE			
unclassified	**unclassified**	**unclassified**	**UU**	**7**	

atoms with each other. These interactions can be split into two categories: bonded and non-bonded. Bonded interactions account for the conformational structure of the molecule, and include bond stretching, bond bending and torsional rotation around the various bonds. These interactions are typically described by harmonic or cosine series potentials, with parameters fit to reproduce quantum chemical data, such as vibrational frequencies and rotational barriers. Non-bonded interactions include van der Waals and electrostatic, which are represented in this work by Lennard-Jones potentials combined with point charges. While bonded parameters are generally fit to quantum chemical data, non-bonded interactions are typically fit to reproduce experimentally measured quantities, such as liquid densities and heats of vaporization.

2.1 Non-bonded interactions

Non-bonded interactions between atoms in each molecule were represented with a standard 12-6 Lennard-Jones potential (Proceedings of the physical society, 1931) with a coulombic term for partial charges.

$$U_r = 4\varepsilon_{ij}\left[\left(\frac{\sigma_{ij}}{r_{ij}}\right)^{12} - \left(\frac{\sigma_{ij}}{r_{ij}}\right)^{6}\right] + \frac{q_i q_j}{4\pi\varepsilon_0 r_{ij}}$$

where r_{ij}, ε_{ij}, σ_{ij}, q_i, q_j are the atom-atom separation, LJ well depth, LJ diameter and the partial charges on the atoms *i* and *j*, respectively. ε_0 is the permittivity of vacuum. Initial estimates of the partial charges for each molecule were determined through a CHELPG analysis (Breneman et al., 1990) of ab initio calculations performed at the HF/6-31g+(d,p) level of theory and basis set. This methodology was chosen based on prior calculations for polar molecules such as H_2S [Kamath et al., 2005] and dimethyl ether [Ketko et al., 2007]. During the parameter optimization process, the quantum mechanically derived partial charges were rescaled by a factor of 0.94 to improve the reproduction of experimentally determined octanol-water partition coefficients. Hydrogen atoms bonded to carbon atoms were grouped with carbon atoms to form a single "united-atom". Lennard-Jones parameters σ and ε for each interaction site were transferred from analogous compounds parameterized previously in the development of the TraPPE force field (Martin et al., 1998; Wick et al., 2000; Stubbs et al., 2004; Wick et al., 2005).

Cross interaction parameters for unlike atoms were determined through Lorentz-Berthelot combining rules (Lorentz, 1881; Berthelot, 1898).

$$\sigma_{ij} = \frac{1}{2}\left(\sigma_{ii} + \sigma_{jj}\right) \qquad \varepsilon_{ij} = \sqrt{\varepsilon_{ii}\varepsilon_{jj}}$$

2.2 Bonded interactions

Equilibrium bond lengths and bond angles, when available, were taken from the TraPPE force field. Any missing equilibrium bond lengths or angles were determined from ab initio HF/6-31g+(d,p) calculations. A harmonic term was used to represent interactions due to bond stretching

$$U_{bond} = \frac{k_b}{2}(r - r_0)^2$$

where U_{bond} is the energy due to bond stretching, k_b is the bending constant and r_0 is the equilibrium bond length. Bond angle bending is also represented by a harmonic potential.

$$U_{bend} = \frac{k_\theta}{2}(\theta - \theta_0)^2$$

where U_{bend} is the energy due to bond bending, k_θ is the bending force constant and θ_0 is the equilibrium bond angle. Barriers to rotation about various dihedral angles was controlled through a cosine series fit to ab initio calculations

$$U_{tor} = \sum_{i=1}^{n} c_i(1 + \cos(i\phi - \delta))$$

where c_i, are torsional force constants and δ is the phase angle. All force constants were determined by fitting parameters to reproduce ab initio derived barriers to bond stretching, bond bending and rotation about dihedral angles. These calculations were performed in Gaussian 03 at the HF/6-31g+(d,p) level of theory and basis set, respectively. The ab initio calculations consist of scanning the bond length or angle of interest, while reoptimizing all remaining degrees of freedom. Equilibrium bond lengths and angles were determined through geometry optimization.

3. METHODOLOGY

3.1 Octanol-water partition coefficient

Octanol-water partition coefficient is the ratio of the concentration of a chemical species in octanol and in water at equilibrium. Octanol has been widely used as a surrogate for organic matter such as lipids since it consists of a nonpolar tail group and a polar head group. Octanol-water partition coefficients are of primary importance in the prediction of the bioactivity, bioaccumulation and transport of a particular chemical species. The methodology used in this work to calculate the partition coefficient is a combination of *NPT* molecular dynamics and free energy perturbation (FEP). The FEP method involves slowly transforming solute A to solute B (either A or B is the compound of interest) by scaling the interaction potential through

$$U(\lambda) = \lambda U_B + (1-\lambda)U_A$$

where λ is the scaling parameter and has values between 0 and 1. The Gibbs free energy of transfer is given by

$$\Delta\Delta G_{Tr}\,AB = \Delta G_{Tr}\,B - \Delta G_{Tr}\,A$$

where $\Delta G_{Tr}\,A$ and $\Delta G_{Tr}\,B$ are the free energies for transferring solute A and B between the water and the water-saturated octanol phase respectively. Calculation of these absolute free energies is difficult. However, because the Gibbs free energy is a state function, the relative Gibbs free energies of solvation between two phases can be determined through the construction of a thermodynamic cycle, as illustrated in Fig. 2.

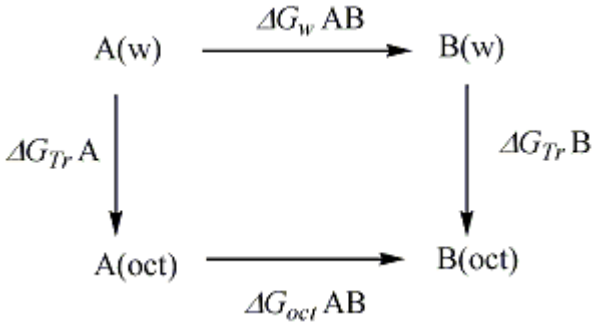

Fig. 2. Thermodynamic cycle utilized to calculate octanol-water partition coefficient.

The thermodynamic cycle provides a means for calculating the relative Gibbs free energy of transfer from the following equation,

$$\Delta\Delta G_{Tr}\,AB = \Delta G_{oct}\,AB - \Delta G_{aq}\,AB$$

where $\Delta G_{Tr(oct)}$ and $\Delta G_{Tr(w)}$ are the free energies associated with the transformation of solute A to solute B in the water-saturated 1-octanol solution and water respectively. The relative partition coefficient is now expressed as

$$\Delta \log K_{ow} = \frac{-\Delta\Delta G_{Tr}\,AB}{2.303RT}$$

The absolute partition coefficient of target molecule B is calculated from the reference molecule A by

$$\log K_{ow}(B) = \Delta \log K_{ow} + \log K_{ow}(A)$$

3.2 Henry's Law Constant

Henry's law constant is the equilibrium distribution of a species between gas and liquid. For dilute aqueous solutions, it is the ratio of the solute's partial pressure and its aqueous concentration. So it provides an estimate for aqueous solubility. Higher Henry's law constant means lower aqueous solubility. Henry's law constant can be expressed in terms of solvation free energy of the solute in water by the following equation (Lin et al., 2002)

$$\log_{10} H_i = \frac{\Delta G_{i/W}^{*sol}}{RT\ln 10} + \log_{10}\frac{RT\rho_w^0}{N_A}$$

where $\Delta G_{i/W}^{*sol}$ is the solvation free energy of species i in solvent water, ρ_W^0 is the number density of pure water and N_A is the avagadro's number. The relative Henry's law constant is determined through MD free energy perturbation from the equation,

$$\Delta \log_{10} H_i = \Delta\Delta G^{sol}$$

where $\Delta\Delta G^{sol}$ is expressed as

$$\Delta\Delta G^{sol} = \frac{\Delta G_w^{sol}(B) - \Delta G_w^{sol}(A)}{2.303RT} = \frac{\Delta G_w(A\to B) - \Delta G_{vac}(A\to B)}{2.303RT}$$

using a thermodynamic path shown in Fig. 3.

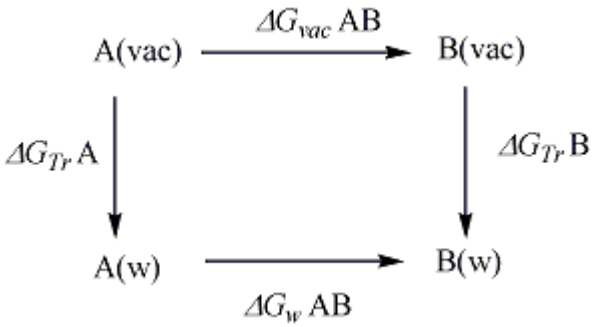

Fig. 3. Thermodynamic path utilized to calculate Henry's law constant.

The absolute constant of B is then calculated from A's Henry's law constant using equation,

$$\log_{10} H(B) = \Delta \log_{10} H - \log_{10} H(A)$$

3.3 Vapor Liquid Equilibria and Vapor Pressure

Gibbs-Duhem integration (Kofke, 1993) is used to determine the phase coexistence curve (temperature vs density) and the vapor pressure. With the knowledge of an initial coexistence point, the Clapeyron equation can be integrated to provide an estimate of coexistence points at other temperatures. The Clapeyron equation is given by

$$\left(\frac{d\ln P}{d\beta}\right)_\sigma = -\frac{\Delta h}{\beta P \Delta v}$$

where P is the pressure, $\beta = 1/kT$, Δh is the difference in molar enthalpies of the coexisting phases, Δv is the difference in molar volumes and σ indicates that the derivative is taken along the saturation line. The method allows for the prediction of the saturation pressure at a temperature ΔT away from a known coexistence point. Given an estimate of the saturation pressure, *NPT*

Molecular Dynamics simulations are performed simultaneously for both liquid and vapor phase to determine the coexistence densities and heat of vaporization. The initial coexistence point in this work was determined by grand canonical histogram reweighting Monte Carlo.

4. SIMULATION DETAILS

4.1 Octanol-water Partition Coefficient

The FEP transformations employed in the calculations are shown in Fig 4.

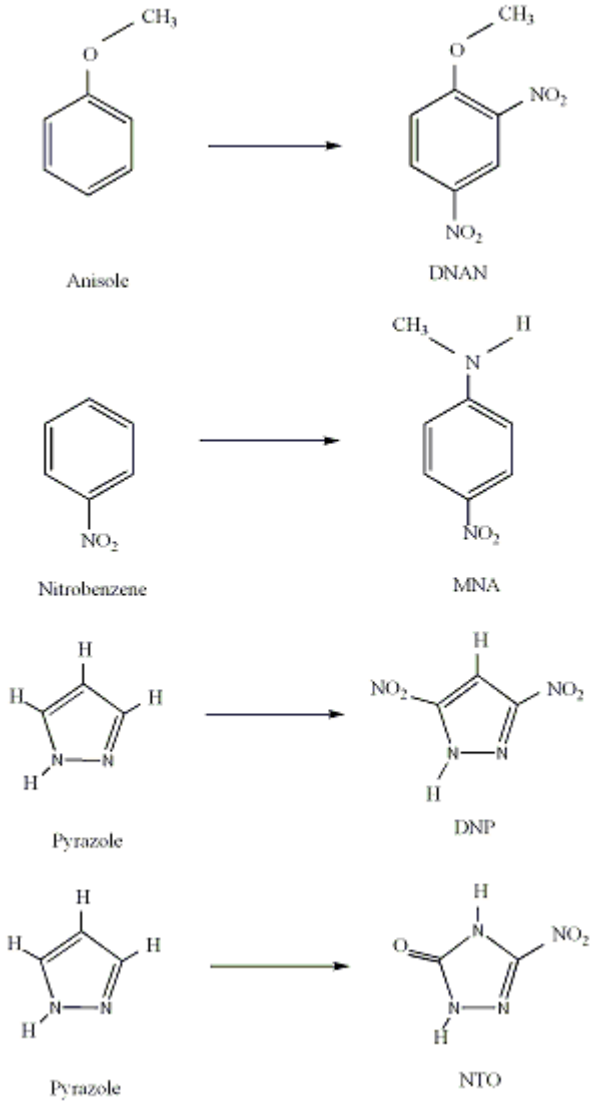

Fig. 4. Schematic of transformations used in the FEP technique.

The reference solutes on the left side of the arrow are slowly transformed to the corresponding target molecules on the right. The choice of the reference solutes depends on structural similarity and availability of experimental partition coefficient data. For each solute of interest, two FEP simulations were performed at 298 K and 1.013 bar; one for the water phase, and the other for water-saturated 1-octanol phase using full periodic boundary conditions. The mole fraction of water in the octanol phase was set to the experimental value of 0.255. Simulations were equilibrated for 1ns (nanosecond) before free energy calculations were initiated. The perturbation was carried out over 20 windows where the starting six and the ending six windows were unequally spaced to improve convergence at the end points. This methodology is known to avoid the so-called end-point catastrophes (Beutler et al., 1994; Pitera et al., 2002) resulting from the appearing and disappearing atoms. After equilibration, FEP calculations were run for a total of 6 ns with 100 ps (picosecond) of equilibration and 100 ps of sampling for each window using a timestep of 1fs. Calculations were performed in the *NPT* ensemble using the FEP module in NAMD. The Langevin piston Nose-Hoover method (Martyna et al., 1994; Feller et al., 1995) was used to control pressure and temperature. A non-bonded cut-off of 14 Å is used for all solutes. Electrostatic interactions were calculated with the particle mesh Ewald technique. The TraPPE-UA (Chen et al., 2001) force field was used to model 1-octanol while the SPC/E (Mark et al., 2001) force field was used to model water.

4.2 Henry's Law constant

The transformation and the FEP scheme used for octanol-water partition coefficient were also used for Henry's law constant calculations. Two simulations, one for the mutation in water and one in vacuum were run at 298 K and 1.013 bar. Simulations in water used the same parameters as the FEP calculations discussed in the previous section. For the calculations in vacuum (*in vacuo*), an isolated hybrid molecule was simulated without periodic boundary conditions and a damping coefficient of 10 ps^{-1} for Langevin temperature control. The vacuum run is carried out for a total of 2.4 ns with 400 ps of equilibration and 2 ns of sampling. The *in vacuo* simulations require longer sampling times. A non-bonded cut-off of 14 Å is used for all the solutes.

4.3 Vapor Liquid Equilibria and Vapor Pressure

One phase coexistence point near the critical temperature was determined through Grand Canonical Monte Carlo (GCMC) simulations coupled with histogram reweighting technique (Ferrenberg et al., 1988; Ferrenberg et al., 1989; Potoff et al., 1998). The insertion of molecules in the GCMC simulations was enhanced through multiple first bead insertions (Esselink et al., 1995) and the application of the coupled-decoupled configurational-bias monte carlo method (Martin et al., 1999; Martin et al., 2006; Wick et al., 2000). The ratios of attempted moves were set to 60% particle insertions/deletions, 10% configurational-bias

regrowths, 15% translations and 15% rotations. A non-bonded cut-off 14 Å was used. No tail corrections were employed for GCMC calculations. Treating this coexistence point as the initial state, Gibbs-Duhem integration is performed to generate the whole phase diagram. Given an estimate of the saturation pressure, *NPT* Molecular Dynamics (MD) simulations are performed simultaneously for both liquid and vapor phase to determine the coexistence densities, heat of vaporization and subsequently the clapeyron equation is integrated to determine pressure. The Langevin piston Nose-Hoover method was used to control pressure and temperature. A non-bonded cut-off of 14 Å was used for all the simulations to maintain consistency with GCMC.

5. RESULTS

5.1 Octanol-Water Partition Coefficients

The partial charges of DNAN and MNA determined from Gaussian 03 were scaled by a factor of 0.94 to fit the experimental octanol-water partition coefficients. Experimental octanol-water partition coefficients for the reference solutes were obtained from the literature (Schultz, 1999; Schultz, 1982). Since no experimental data exists for either DNP or NTO, the same charge scheme was applied to these materials. The partition coefficients predicted by the FEP method are presented in Table 1 alongside values predicted by Toghiani et al. (Toghiani et al., 2008) through group contribution (Broto et al., 1984) and COSMOthermX software and the experimental data (Boddu et al, 2008; Boddu et al, 2008). The octanol-water partition coefficients predicted for DNAN and MNA are in very good agreement with the experimental values. The values predicted for DNP and NTO compare well with the group contribution values but slightly deviate from COSMOtherm predictions.

TABLE 1. PREDICTED OCTANOL-WATER PARTITION COEFFICIENT (LOG K_{OW})

Compound	FEP	Group Contribution	COSMO thermX	Exp
DNAN	1.78	1.70	1.92	1.64
MNA	2.02	1.57	0.80	2.04
DNP	-0.65	-0.82	-1.19	-
NTO	1.03	0.9	0.37	-

5.2 Henry's Law Constants

Henry's law constants predicted for the newly developed force fields for DNAN, MNA, DNP and NTO are shown in Table 2. The Henry's law constants for the reference molecules were obtained from the literature (Hine et al., 1974). No direct Henry's law constant has been reported in literature for pyrazole although we were able to calculate that using the relation

$$H = p / S$$

where p is the vapor pressure and S is the solubility in water at 298 K. The vapor pressure of pyrazole at 298 K is 3.638 Pa (Jimenez et al., 1987) and the solubility in water at 298 K is 19.4 mol/kg of water (Wiley, 1967).

TABLE 2. PREDICTED HENRY'S LAW CONSTANTS (LOG H)

Compound	FEP	Exp
DNAN	-4.40	-3.25
MNA	-3.84	-3.60
DNP	-6.59	-
NTO	-11.38	-

While DNAN Henry's law constant deviates slightly from the experiment, the value predicted for MNA agrees well with the experiment.

5.3 Vapor Liquid Equilibria and Vapor Pressure

The phase coexistence curve and the Clausius-Clapeyron plot generated through Gibbs-Duhem integration are shown in Fig 5 & 6 respectively.

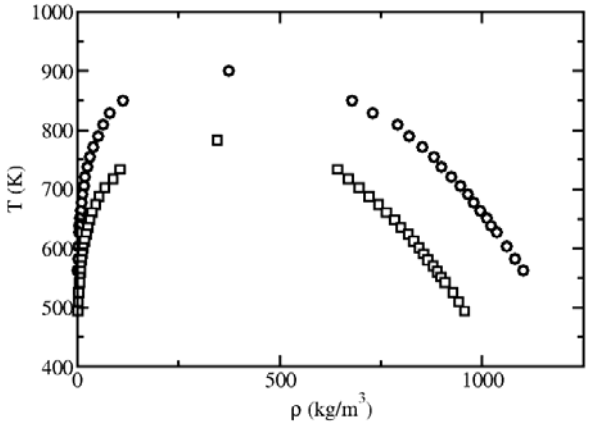

Fig. 5. Vapor liquid equilibria of DNAN (circle) and MNA (square)

Critical temperatures and densities are computed by fitting the saturated liquid and vapor densities to the density scaling law for critical temperature (Rowlinson and Widom, 1982)

$$\rho_{liq} - \rho_{vap} = B(T - T_c)^{\beta}$$

and the law of rectilinear diameters (Rowlinson and Swinton, 1982)

$$\frac{\rho_{liq} + \rho_{vap}}{2} = \rho_c + A(T - T_c)$$

where $\beta = 0.325$ is the critical exponent for Ising-type fluids in three dimensions (Privman et al., 1998) and *A* and *B* are constants fit to simulation data.

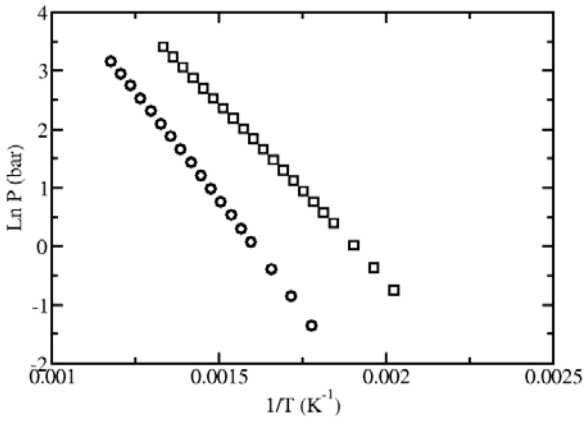

Fig. 6. Clausius-Clapeyron plot of DNAN (circle) and MNA (square)

Normal boiling points and critical pressures were determined from the Clausius-Clapeyron plots through linear-interpolation. The critical parameters and the normal boiling point are presented in Table 3.

TABLE 3. PREDICTED CRITICAL PARAMETERS AND BOILING POINT FOR DNAN AND MNA

Compound	**T_c (K)**	**ρ_c (kg/m^3)**	**P_c (bar)**	**T_b (K)**
DNAN	900.01	40.33	374.54	623.75
MNA	783.47	48.45	345.99	511.90

No experimental data exists for either DNAN or MNA to make a comparison.

CONCLUSIONS

In this work, we have demonstrated the potential of atomistic computer simulations in the predictions of physical properties and partitioning of insensitive munitions. Such predictive capability may lead to improved cost savings and reduced development time if candidate molecules can be pre-screened on computer before synthesis. Force fields have been presented for DNAN, MNA, DNP and NTO. The predictions of simulation for the octanol-water partition coefficient and Henry's law constant were found to be in good agreement with the spare experimental data available in the open literature.

ACKNOWLEDGEMENTS

Financial support from ERDC-CERL (W9132T-06-2-0027) is greatly appreciated. Part of the computer resources used in this work was provided by the Grid Computing Resource at Wayne State University.

REFERENCES

Beutler, T.C., Mark, A.E., van Schaik, R.C., Gerber, P.R., van Gunsteren, W.F., 1994: Avoiding singularities and neumerical instabilities in free energy calculations based on molecular simulations, *Chem. Phys. Lett*., **222**, 529-539.

Breneman, C.M., Wiberg, K.B., 1990: Determining atom-centered monopoles from molecular electrostatic potentials. The need for high sampling density in formamide conformational analysis, *J.Comp*, *Chem.*, **11,** 361-373.

Boddu, V.M., Abburi, K., Maloney, S.W., Reddy, D., 2008: Thermophysical Properties of an Insensitive Munitions Compound, 2,4-Dinitroanisole, *J. Chem. Eng. Dat*., **53**, 1120-1125.

Boddu, V.M., Abburi, K., Maloney, S.W., Reddy, D., 2008: Physicochemical properties of an insensitive munitions compound, N-methyl-4-nitroaniline (MNA), *J.Hazad. Mat.*, **155**, 288-294.

Broto, P., Moreau, G., Vandycke, C., 1984: Molecular structure: perception, auto-correlation descriptor and sar studies. System of atomic contributions for the calculation of the n-octanol/water partition coefficients, *Eur. J. Med. Chem. Chim. Ther*., **19**, 71-78.

Chen, B., Potoff, J.J., Siepmann, J.I., 2001: Monte Carlo Calculations for Alcohols and Their Mixtures with Alkanes. Transferable Potentials for Phase Equilibria. 5. United-Atom Description of Primary, Secondary, and Tertiary Alcohols, *J. Phys. Chem. B*, **105**, 3093-3104.

Esselink, K., Loyens, L.D.J.C., Smit, B., 1995: Parallel Monte Carlo simulations, Phys. Rev. E, **51**, 1560-1568.

Feller, S.W., Zhang, Y., Pastor, R.W., Brooks, B.R., 1995: Constant pressure molecular dynamics simulation:

The Langevin piston method, *J. Chem. Phys*., **103,** 4613-4621.

Ferrenberg, A.M., Swendsen, R.H., 1988: New Monte Carlo technique for studying phase transitions, *Phys. Rev. Lett,*. **61**, 2635-.2638.

Ferrenberg, A.M., Swendsen, R.H., 1989: New Monte Carlo technique for studying phase transitions, *Phys. Rev. Lett,*. **63**, 1195-1198.

Gillett, J.W., 1983: A comprehensive prebiological screen for ecotoxicologic effects, *Environmental Toxicology and Chemistry*, **2**, 463-476.

Hine, J., Mookerjee, P.K., 1975: The Intrinsic Hydrophilic Character of Organic Compounds. Correlations in Terms of Structural Contributions, *J. Org. Chem.,* **40,** 292-298.

Jimenez, P., Roux, M.V., Turrion, C., 1987: Thermochemical properties of N-heterocyclic compounds I. Enthalpies of combustion, vapor pressures and enthalpies of sublimation and enthalpies of formation of pyrazole, imidazole, indazole and benzimidazole, *J. Chem. Thermodynamics.*, **19**, 985-992.

Kamath, G., Lubna, N., Potoff, J.J., 2005: Effect of partial charge parametrization on the fluid phase behavior of hydrogen sulfide, *J. Chem. Phys.*, **12**, 124505-124512.

Ketko, M.B.H., Potoff, J.J., 2007: Effect of partial charge parametrization on the phase equilibria of dimethyl ether, *Mol. Sim.*, **33**, 769-776.

Kofke, D.A., 1993: Direct evaluation of phase coexistence by molecular simulation via integration along the saturation line, *J.Chem. Phys*., **98**, 4149-4162.

Lin, S.-T., Sandler, S.I., 2002: Henry's law constant of organic compounds in water from a group contribution model with multipole corrections, *Chemical Engineering Science*, **57,** 2727-2733**.**

Martin, M.G., Siepmann, J.I., 1998: Transferable Potentials for Phase Equilibria. 1. United-Atom Description of *n*-Alkanes, *J. Phys. Chem. B,* **102**, 2569-2577.

Martin, M.G., Siepmann, J.I., 1999: Novel Configurational-Bias Monte Carlo Method for Branched Molecules. Transferable Potentials for Phase Equilibria. 2. United-Atom Description of Branched Alkanes, *J. Phys. Chem. B,* **103,** 4508-4517.

Martin, M.G., Frischknecht, A.L., 2006: Using arbitrary trial distributions to improve intramolecular sampling in configurational-bias Monte Carlo, *Mol. Phys*., **104,** 2439-2456.

Martyna, G.J., Tobias, D.J., Klein, M.L., 1994: Constant Pressure Molecular Dynamics Algorithms, *J. Chem. Phys.*, **101**, 4177-4189.

Privman, V., Trigg, G.L., 1998, *Encyclopedia of Applied Physics*., Wiley-VCH, Berlin, **23,** 41.

Pitera, J.W., van Gunsteren., W.F., 2002: A comparison of non-bonded scaling approaches for free energy calculations, *Mol. Sim.*, **28,** 45-65.

Rowlinson, J.S., Widom, B., 1982, *Molecular Theory of Capillarity*, Clarendon Press, Oxford.

Rowlinson, J.S., Swinton, F.L., 1982, *Liquids and Liquid Mixtures*, 3rd edn., Butterworth.

Sanster, J., 1997: *Octanol-Water Partition Coefficients: Fundamentals and Physical Chemistry*, Vol. 2 of Wiley Series in Solution Chemistry, John Wiley & Sons Ltd.

Schultz, T.W., 1999: Structure-toxicity relationships for benzenes evaluated with Tetrahymena pyriformis, *Chemical Research in Toxicology*, **12**, 1262-1267.

Schultz, T.W., Cajina-Quezada, M., 1982: Structure-toxicity Relationships of Selected Nitrogenous Heterocyclic Compounds II. Dinitrogen Molecules, *Arch.Environ.Contam.Toxicol*., **11**, 353-361.

Stubbs, J.M., Potoff, J.J., Siepmann, J.I., 2004: Transferable Potentials for Phase Equilibria. 6. United-Atom Description for Ethers, Glycols, Ketones, and Aldehydes, *J. Phys. Chem. B,* **108,** 17596-17605.

Wick, C.D., Martin, M.G., Siepmann, J.I., 2000: Transferable Potentials for Phase Equilibria. 4. United-Atom Description of Linear and Branched Alkenes and Alkylbenzenes, *J.Phys.Chem. B,* **104,** 8008-8016.

Wick, C.D., Stubbs, J.M., Rai, N., Siepmann, J.I., 2005: Transferable Potentials for Phase Equilibria. 7. Primary, Secondary, and Tertiary Amines, Nitroalkanes and Nitrobenzene, Nitriles, Amides, Pyridine, and Pyrimidine, *J. Phys. Chem. B*, **109,** 18974-18982.

Wiley, R.H., 1967, *Pyrazoles, pyrazolines, pyrazolidines, indazoles and condensed rings*, Interscience Publishers, New York.